Supporting Information for

$KTeOPO_4$ and $NH_4SnClSO_4$: Two New $KTiOPO_4$ Derivatives as Birefringent Crystals Featuring Enhanced Optical Anisotropy

Ruonan Zhang,[a,b] Xuping Shi,[a,b] Abudukadi Tudi,[a,b] Wenbin Zhang,[a,b] Zhihua Yang,[a,b] Fangfang Zhang,[a,b] Shilie Pan,[a,b]* Shujuan Han[a,b]*

[a]Research Center for Crystal Materials; CAS Key Laboratory of Functional Materials and Devices for Special Environmental Conditions; Xinjiang Technical Institute of Physics and Chemistry, CAS, 40-1 South Beijing Road, Urumqi 830011, China.

[b]Center of Materials Science and Optoelectronics Engineering, University of Chinese Academy of Sciences, Beijing 100049, China

*E-mails: slpan@ms.xjb.ac.cn, hansj@ms.xjb.ac.cn.

Experimental Section

Synthesis.

TeI_4 (≥ 99%), KH_2PO_4 (≥ 99.5%), $LiNO_3$ (≥ 99%), K_2CO_3 (99%), $NH_4H_2PO_4$ (≥ 99%), TeO_2 (≥ 99%), $(NH_4)_2SO_4$ (≥ 99%), $SnCl_2$ (≥ 98%) and $SnSO_4$ (AR) were purchased from Aladdin and used as received.

Crystals of $KTeOPO_4$ were grown in a closed system, the mixture of TeI_4, KH_2PO_4 and $LiNO_3$ with the molar ratio 1: 4: 1 was loaded into a clean quartz tube, which was washed using deionized water and dried at a high temperature. Then the tube was flame-sealed under 10^{-3} Pa and heated at 400 ℃ for 20 h. Subsequently, the temperature was decreased to 200 ℃ at a rate of 1 ℃/h, and finally cooled to room temperature at a rate of 10 ℃/h. The transparent crystals were separated for structural determination. Polycrystalline samples of $KTeOPO_4$ were synthesized by a conventional solid-state reaction method. And the preparation process is as follows: the raw materials of K_2CO_3, $NH_4H_2PO_4$ and TeO_2 at a ratio of 1: 2: 2 were thoroughly ground and placed in an alumina crucible. Then the crucible was heated at about 190 ℃ for 4 days with several intermittent grindings.

$NH_4SnClSO_4$ crystals were grown by hydrothermal method. The mixture of $(NH_4)_2SO_4$ (0.246 g, 1.862 mmol), $SnCl_2$ (0.353 g, 1.862 mmol) and $SnSO_4$ (0.400 g, 1.862 mmol) were added with deionized water (0.8 mL) and mixed homogeneously. The mixture was transferred into 23 mL Teflon-lined autoclaves, and the autoclaves were heated to 200 ℃ for 3 days, then cooled down to room temperature. The block crystals were obtained (Fig. S5). And the polycrystalline of $NH_4SnClSO_4$ is easily to get from the above process.

Single-Crystal X-ray Diffraction

The single-crystal XRD data were collected on a Bruker D8 Venture diffractometer assembled with monochromatic Mo-Kα (λ = 0.71073 Å) as the radiation source at room temperature and then integrated by using the SAINT program[1]. All the structures were solved by direct methods and refined through the full-matrix least-squares fitting on F2 with the OLEX2 software[2]. These structures were verified utilizing the ADDSYM algorithm from PLATON[3]. Crystallographic data and structural refinements for the title compounds are summarized in Table S1. The final refined atomic positions and isotropic thermal parameters, selected bond lengths, and angles for the title compounds are given in Tables S2–S5. The structural rationality of the two compounds is also evident from bond valence sum (BVS) calculations (Tables S2−S3).

Powder X-ray Diffraction

Powder X-ray diffraction (XRD) pattern has been measured to verify the phase-purity of the polycrystalline sample for $KTeOPO_4$ and $NH_4SnClSO_4$. Powder XRD data were collected with a Bruker D2 PHASER diffractometer equipped with Cu Kα radiation (λ = 1.5418 Å) at room temperature. Data were collected in the angular (2θ) ranging from 10 to 70 ° with a scan step width and a fixed counting time of 0.02 ° and 1 s/step, respectively. The experimental XRD patterns are presented in Fig. S6, which are consistent with the calculated patterns fitted from single-crystal X-ray diffraction, confirming that the powder samples are pure phases. However, a small amount of TeO_2 impurity persisted in $KTeOPO_4$ powder samples and was difficult to eliminate completely.

Energy Dispersive X-ray (EDX) Spectroscope

EDX spectroscope was measured on a SUPRA 55VP field emission scanning electron microscope equipped with a BRUKER X-ray Flash-SDD-5010 energy-dispersive X-ray spectroscope. The EDX results verify the existence of the element K, Te, P and O for $KTeOPO_4$ and N, Sn, S, O and Cl for $NH_4SnClSO_4$, respectively (Figs. S3a and 3b).

Thermal Analysis

Thermogravimetric analyses (TGA) and differential scanning calorimetry (DSC) were measured on a NETZSCH STA 449 F3 simultaneous analyzer instrument. The polycrystalline powders were placed in a Pt crucible and heated from room temperature to 800 °C or 500 °C at a rate of 5 °C·min^{-1} under a constant flow of nitrogen gas. The thermal behaviors of $KTeOPO_4$ and $NH_4SnClSO_4$ are presented in Fig. S7. It can be seen that $NH_4SnClSO_4$ begins to decompose at approximately 243 ℃, accompanied by significant weight loss. And the endothermic peak at 447 ℃ may be the melting point of the decomposition product, indicating that $NH_4SnClSO_4$ melts incongruently. There is only one endothermic peak at the DSC curve of $KTeOPO_4$, suggesting that it may be a congruent compound. To further investigate the melting behavior of $KTeOPO_4$, its polycrystalline powder was sintered at 220 ℃. The XRD patterns of the sintered sample differ from the calculated ones (Fig. S6a), which indicates that $KTeOPO_4$ also melts incongruently.

Infrared Spectroscopy

The infrared spectra were recorded using a Shimadzu IRAffinity-1 Fourier transform infrared spectrometer within the range of 400–4000 cm^{-1}. The sample was mixed with dried KBr.

UV−Vis−NIR Diffuse Reflectance Spectroscopy

The diffuse reflectance spectra were measured by using a Shimadzu Solid Spec-3700 DUV spectrophotometer in the wavelength range of 200–2600 nm at room temperature.

Birefringence Measurement

The birefringence of $NH_4SnClSO_4$ was characterized by using the polarizing microscope equipped (ZEISS Axio Scope A1) with Berek compensator[4]. The wavelength of the light source was 546 nm. The formula for calculating the birefringence is listed below:

$$R = |N_g - N_p| \times T = \Delta n \times T \quad (1)$$

Herein, R represents the optical path difference; N_g, N_p, and Δn mean the refractive indices of fast light, slow light, and the birefringence, respectively; T denotes the thickness of the crystal. The $NH_4SnClSO_4$ crystal was not grown along the optical principal axis direction, so only the refractive index difference is obtained from birefringence measurement. The optical principal axis direction of $NH_4SnClSO_4$ crystal is [0.0084331, 0.0000000, 0.0437969], [-0.0000001, -0.2136524, 0.0000000], [0.1706056, -0.0000001, 0.0001920].

Computational Methods

The electronic structure and optical properties of compounds were obtained by using the pseudopotential plane-wave method based on CASTEP package[5]. The generalized gradient approximation (GGA)[6] with the Perdew-Burke-Ernzerhof (PBE) functional[7] was used to describe the exchange-correlation potential, with an energy cutoff of 750.0 eV. The Brillouin zone was sampled using a 6 × 7 × 1 Monkhorst−Pack k-point grid with a separation of 0.03/Å. Norm-conserving pseudopotentials were utilized for each atomic species, with the following valence configurations: K $3s^2$ $3p^6$ $4s^1$, Te $5s^2$ $5p^4$, P $3s^2$ $3p^3$, S $3s^2$ $3p^4$, N $2s^2$ $2p^3$, H $1s^1$, O $2s^2$ $2p^4$, Cl $3s^2$ $3p^5$, Sn $5s^2$ $5p^2$, and F $2s^2$ $2p^5$.

The linear optical properties were obtained by calculating the dielectric function with following formula:

$$\varepsilon(\omega) = \varepsilon_1(\omega) + i\varepsilon_2(\omega) \tag{2}$$

in which $\varepsilon_1(\omega)$ and $\varepsilon_2(\omega)$ are the real and imaginary parts of the dielectric function respectively. $\varepsilon_2(\omega)$ was obtained by the following formula:

$$\varepsilon_2(\omega) = \frac{4\pi l^2}{\Omega}\lim_{q\to 0}\frac{1}{q^2}\times\sum_{c,v,k} 2\omega_k\delta(E_c - E_v - \omega)\,|\langle c\,|\,e\cdot q\,|\,v\rangle|^2 \tag{3}$$

where $\langle c\,|\,e\cdot q\,|\,v\rangle$ is the integrated optical transitions from the valance states (v) to the conduction states (c), *e*, *q* express the polariozation direction of the photon and electron momentum operator. The Kramers-Kroning transform was used for calculating the real part of the dielectric $\varepsilon_1(\omega)$ from $\varepsilon_2(\omega)$. Finally， the refractive index *n*(□) and birefringence (Δ*n*) can be calculated.

Table S1. Crystal data and structure refinement for $KTeOPO_4$ and $NH_4SnClSO_4$.

Empirical formula	$KTeOPO_4$	$NH_4SnClSO_4$
Formula weight	277.67	268.24
Temperature	300 K	299 K
Wavelength	0.71073 Å	0.71073 Å
Crystal system, space group	Monoclinic, $P2_1/c$	Monoclinic, $P2_1/c$
Unit cell dimensions	a = 5.4471(8) Å	a = 5.8628(3) Å
	b = 10.3373(14) Å β = 95.229(7)°	b = 4.6805(2) Å β = 93.081(2)°
	c = 8.9393(12) Å	c = 22.8655(11) Å
Volume	501.26(12) Å^3	626.54(5) Å^3
Z, Calculated density	4, 3.679 g/cm^3	4, 2.844 g/cm^3
Absorption coefficient	7.008 mm^{-1}	4.770 mm^{-1}
F(000)	504	504
ϑ range for data collection	3.020 to 27.329°	3.480 to 27.500°
Limiting indices	-7 ≤ h ≤ 7, -13 ≤ k ≤ 13, -11 ≤ l ≤ 11	-7 ≤ h ≤ 7, -6 ≤ k ≤ 6, -29 ≤ l ≤ 29
Reflections collected / unique	6501 / 1105 [R(int) = 0.0658]	14360 / 1437 [R(int) = 0.0638]
Completeness	98.60	99.80
Maximum and minimum transmission	0.7455 and 0.5649	0.7456 and 0.6689
Refinement method	Full matrix least squares on F^2	Full matrix least squares on F^2
Data / restraints / parameters	1105 / 0 / 74	1437 / 19 / 85
Goodness-of-fit on F^2	1.142	1.140
Final R indices [$F_o^2 > 2\sigma(F_o^2)$][a]	R_1 = 0.0328, wR_2 = 0.0713	R_1 = 0.0244, wR_2 = 0.0481
R indices (all data)[a]	R_1 = 0.0408, wR_2 = 0.0788	R_1 = 0.0301, wR_2 = 0.0520
Largest diff. peak and hole	1.230 and −0.957 e·Å^{-3}	0.586 and -0.594 e·Å^{-3}

[a] $R_1 = \Sigma||F_o| - |F_c||/\Sigma|F_o|$ and $wR_2 = [\Sigma w(F_o^2 - F_c^2)^2/\Sigma wF_o^4]^{1/2}$ for $F_o^2 > 2\sigma(F_o^2)$

Table S2. Atomic coordinates (× 10^4) and equivalent isotropic displacement parameters (Å^2 × 10^3) for $KTeOPO_4$. U_{eq} is defined as one-third of the trace of the orthogonalized U_{ij} tensor.

atoms	x	y	z	U_{eq}	BVS
K(1)	2980(3)	6625(1)	5551(2)	28(1)	1.11
Te(1)	11725(1)	4220(1)	1092(1)	17(1)	4.23
P(1)	7927(3)	6242(2)	2570(2)	19(1)	4.92
O(1)	5784(10)	5999(5)	3441(7)	35(1)	-1.83
O(2)	9545(9)	7409(4)	3161(6)	28(1)	-2.04
O(3)	7038(9)	6523(5)	897(6)	26(1)	-2.31
O(4)	9736(9)	5056(4)	2720(5)	21(1)	-2.00
O(5)	8550(8)	4075(4)	0(6)	19(1)	-2.08

Table S3. Atomic coordinates (× 10^4) and equivalent isotropic displacement parameters (Å^2 × 10^3) for $NH_4SnClSO_4$. U_{eq} is defined as one-third of the trace of the orthogonalized U_{ij} tensor.

Atoms	x	y	z	U_{eq}	BVS
Sn(1)	2757(1)	1795(1)	7043(1)	22(1)	1.79
S(1)	2706(2)	6354(2)	6013(1)	21(1)	6.10
Cl(1)	-1532(2)	2069(3)	6950(1)	34(1)	-0.75
O(1)	2778(5)	3180(6)	6115(1)	27(1)	-1.85
O(3)	612(5)	7093(7)	5692(1)	36(1)	-2.01
O(4)	4679(5)	7183(6)	5701(1)	36(1)	-1.65
O(2)	2796(5)	7581(6)	6615(1)	31(1)	-1.63
N(1)	7593(6)	12019(7)	5536(2)	28(1)	–

Table S4. Selected bond lengths (Å) and angles (deg.) for $KTeOPO_4$.

K(1)-O(1)#4	2.917(6)	Te(1)-O(4)	2.080(5)
K(1)-O(1)	2.614(6)	Te(1)-O(5)	1.913(5)
K(1)-O(2)#5	3.277(6)	Te(1)-O(5)#6	2.014(4)
K(1)-O(2)#2	2.827(6)	Te(1)-O(3)#6	2.104(5)
K(1)-O(4)#4	2.831(5)	P(1)-O(1)	1.483(6)
K(1)-O(4)#2	3.367(5)	P(1)-O(2)	1.558(5)
K(1)-O(5)#1	2.698(4)	P(1)-O(4)	1.571(5)
K(1)-O(3)#3	2.920(5)	P(1)-O(3)	1.556(5)
Te(1)-O(2)#7	2.124(4)		
O(1)-K(1)-O(1)#4	81.91(18)	O(5)#1-K(1)-O(2)#5	69.94(13)
O(1)#4-K(1)-O(2)#5	101.19(14)	O(5)#1-K(1)-O(4)#4	120.53(14)
O(1)-K(1)-O(2)#2	85.17(18)	O(5)#1-K(1)-O(4)#2	100.53(13)
O(1)-K(1)-O(2)#5	176.57(15)	O(5)#1-K(1)-O(3)#3	67.79(14)
O(1)#4-K(1)-O(4)#2	82.83(15)	O(3)#3-K(1)-O(2)#5	101.57(14)
O(1)-K(1)-O(4)#2	68.89(16)	O(3)#3-K(1)-O(4)#2	137.38(14)
O(1)-K(1)-O(4)#4	127.65(16)	O(4)-Te(1)-O(2)#7	86.62(19)
O(1)-K(1)-O(5)#1	106.96(17)	O(4)-Te(1)-O(3)#6	166.07(18)
O(1)-K(1)-O(3)#3	75.65(17)	O(5)-Te(1)-O(2)#7	77.65(18)
O(1)#4-K(1)-O(3)#3	115.18(16)	O(5)#6-Te(1)-O(2)#7	155.71(19)
O(2)#2-K(1)-O(1)#4	128.20(17)	O(5)#6-Te(1)-O(4)	87.43(18)
O(2)#2-K(1)-O(2)#5	93.97(13)	O(5)-Te(1)-O(4)	83.40(19)
O(2)#5-K(1)-O(4)#2	112.79(13)	O(5)-Te(1)-O(5)#6	78.28(19)
O(2)#2-K(1)-O(4)#2	45.94(12)	O(5)#6-Te(1)-O(3)#6	85.70(19)
O(2)#2-K(1)-O(4)#4	104.24(15)	O(5)-Te(1)-O(3)#6	83.3(2)
O(2)#2-K(1)-O(3)#3	109.55(14)	O(3)#6-Te(1)-O(2)#7	94.7(2)
O(4)#4-K(1)-O(1)#4	51.54(14)	O(1)-P(1)-O(2)	113.7(3)
O(4)#4-K(1)-O(2)#5	55.78(12)	O(1)-P(1)-O(4)	109.9(3)
O(4)#4-K(1)-O(4)#2	81.38(14)	O(1)-P(1)-O(3)	110.2(3)

O(4)#4-K(1)-O(3)#3	140.61(15)	O(2)-P(1)-O(4)	104.1(3)
O(5)#1-K(1)-O(1)#4	171.12(16)	O(3)-P(1)-O(2)	107.3(3)
O(5)#1-K(1)-O(2)#2	54.59(13)	O(3)-P(1)-O(4)	111.5(3)

Symmetry transformations used to generate equivalent atoms:

#1 -x+1,y+1/2,-z+1/2 #2 x-1,y,z #3 x,-y+3/2,z+1/2

#4 -x+1,-y+1,-z+1 #5 x-1,-y+3/2,z+1/2 #6 -x+2,-y+1,-z

#7 -x+2,y-1/2,-z+1/2

Table S5. Selected bond lengths (Å) and angles (deg.) for $NH_4SnClSO_4$.

Sn(1)-Cl(1)	2.5149(11)	S(1)-O(3)	1.439(3)
Sn(1)-O(1)	2.218(3)	S(1)-O(4)	1.444(3)
Sn(1)-O(2)#1	2.203(3)	S(1)-O(2)	1.489(3)
S(1)-O(1)	1.504(3)		
O(1)-Sn(1)-Cl(1)	87.75(8)	O(3)-S(1)-O(2)	111.45(19)
O(2)#1-Sn(1)-Cl(1)	92.42(9)	O(4)-S(1)-O(1)	109.04(17)
O(2)#1-Sn(1)-O(1)	80.54(10)	O(4)-S(1)-O(2)	111.27(19)
O(3)-S(1)-O(1)	109.46(18)	O(2)-S(1)-O(1)	103.72(16)
O(3)-S(1)-O(4)	111.6(2)		

Symmetry transformations used to generate equivalent atoms:

#1 x,y-1,z

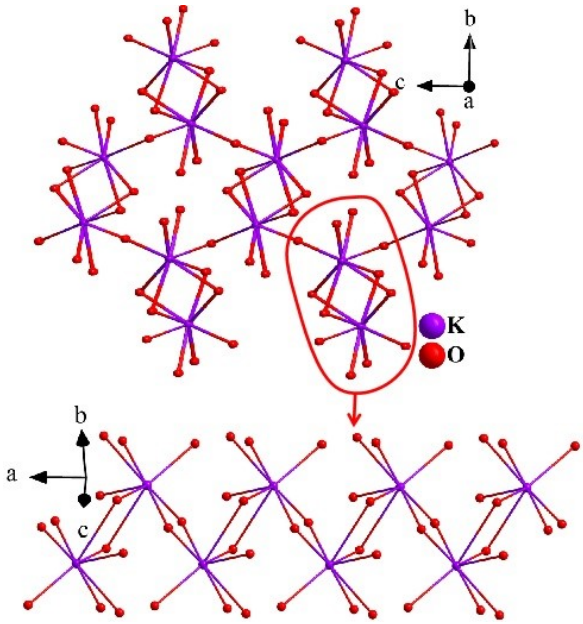

Fig. S1. The coordination and connection of K atoms in $KTeOPO_4$.

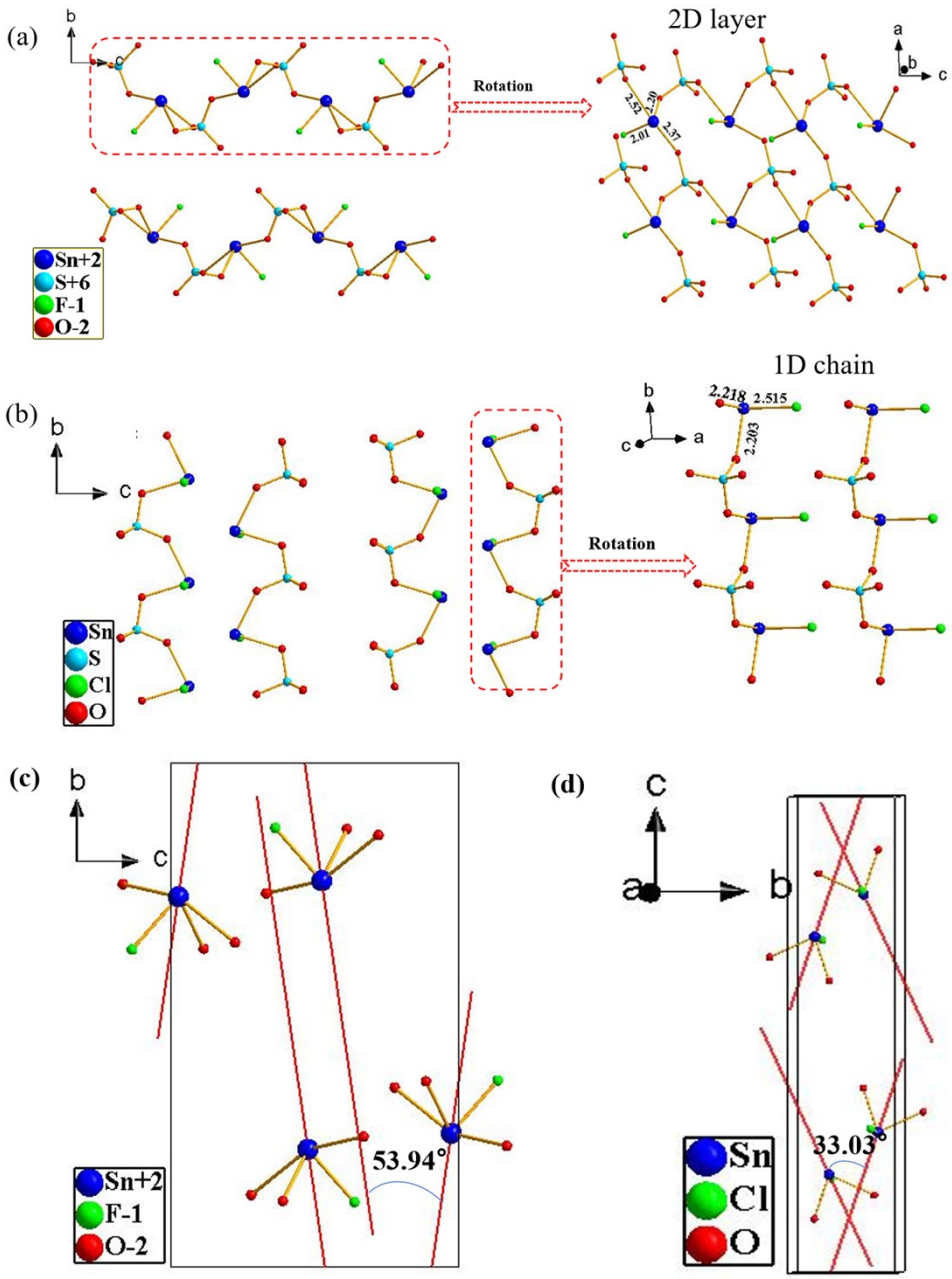

Fig. S2. (a) The 2D layer formed by [SO_4] and [SnO_3F]; (b) The 1D chain formed by [SO_4] and [SnO_2Cl]; (c) The arrangement of lone-pair electrons in the unit cell of NH_4SnFSO_4; (d) The arrangement of lone-pair electrons in the unit cell of $NH_4SnClSO_4$.

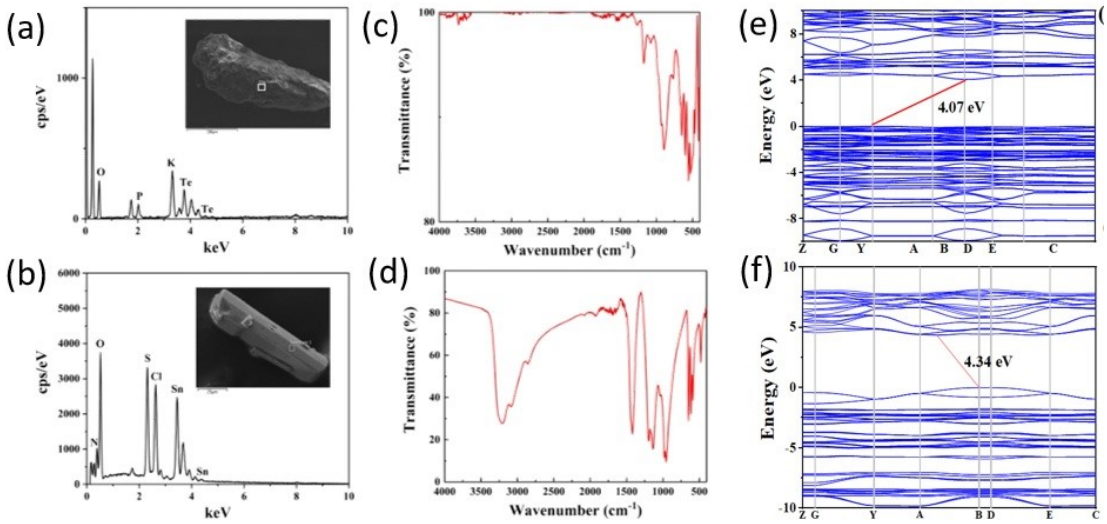

Fig. S3. (a, b) Energy dispersive X-ray spectroscopes for $KTeOPO_4$ and $NH_4SnClSO_4$; (c, d) IR spectra for $KTeOPO_4$ and $NH_4SnClSO_4$; (e, f) Calculated band structures for $KTeOPO_4$ and $NH_4SnClSO_4$.

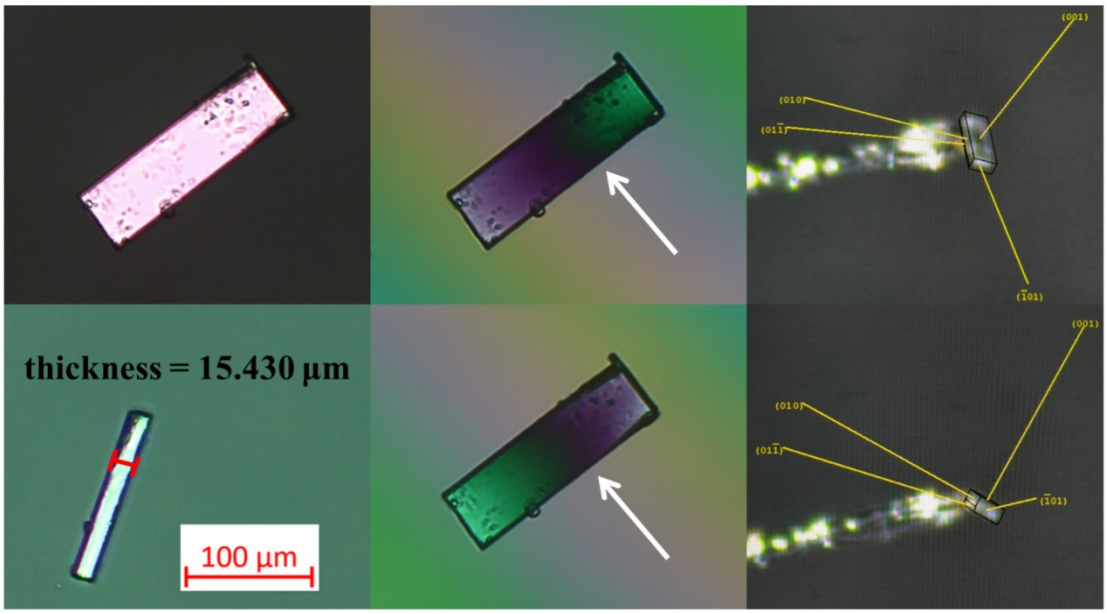

Fig. S4. Birefringence measurement of $NH_4SnClSO_4$.

Fig. S5. The photograph of $NH_4SnClSO_4$ crystal.

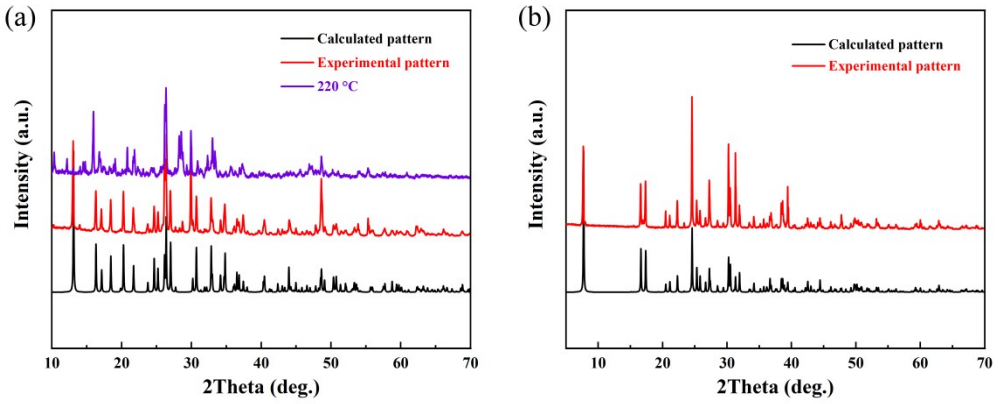

Fig. S6. Experimental and calculated powder XRD patterns for $KTeOPO_4$ and $NH_4SnClSO_4$.

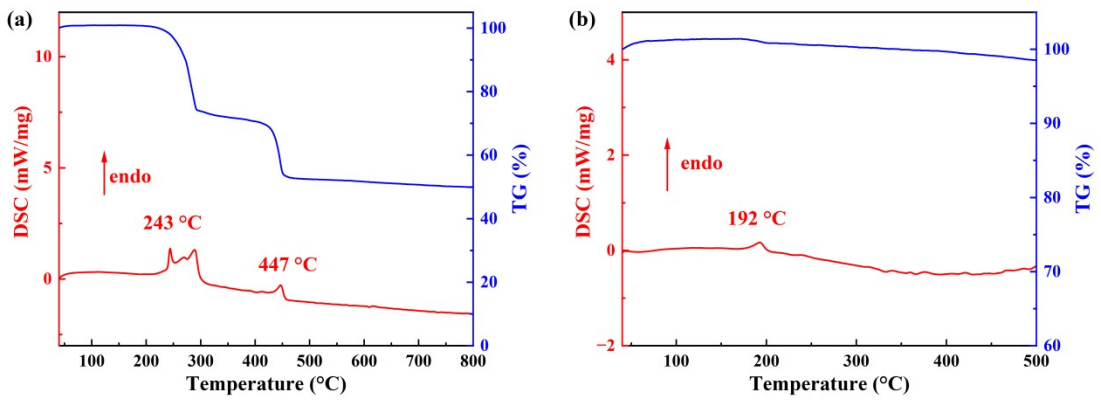

Fig. S7. DSC-TG curves for (a) $NH_4SnClSO_4$ and (b) $KTeOPO_4$, respectively.

References

1. SAINT, version 7.60A, Bruker Analytical X-ray Instruments, Inc., Madison, WI, 2008.

2. O. V. Dolomanov, L. J. Bourhis, R. J. Gildea, J. A. K. Howard and H. Puschmann, : a complete structure solution, refinement and analysis program, J Appl Crystallogr, 2009, 42, 339–341.

3. A. L. Spek, Single-crystal structure validation with the program, J Appl Crystallogr, 2003, 36, 7–13.

4. L. L. Cao, G. Peng, W. B. Liao, T. Yan, X. F. Long and N. Ye, A microcrystal method for the measurement of birefringence, Crystengcomm, 2020, 22, 1956–1961.

5. S. J. Clark, M. D. Segall, C. J. Pickard, P. J. Hasnip, M. J. Probert, K. Refson and M. C. Payne, First principles methods using CASTEP, Z Kristallogr, 2005, 220, 567–570.

6. J. P. Perdew, K. Burke and M. Ernzerhof, Generalized gradient approximation made simple, Physical Review Letters, 1996, 77, 3865–3868.

7. A. M. Rappe, K. M. Rabe, E. Kaxiras and J. D. Joannopoulos, Optimized Pseudopotentials, Physical Review B, 1990, 41, 1227–1230.